# Increased co-oxidation activity for mercury under hot and cold site coal power plant conditions – Preparation and evaluation of Au/TiO$_2$-coated SCR-DeNO$_x$ catalysts

Beatrice-Andreea Dranga [a],[b],[*], Heinz Koeser [c],[**]

[a] Martin-Luther University Halle-Wittenberg, Centre for Engineering Science, D-06099 Halle (Saale), Germany
[b] Gheorghe Asachi Technical University of Iasi, Faculty of Chemical Engineering and Environmental Protection, 73 Prof. Dr. Mangeron Street, Iasi 700050, Romania
[c] Otto-von-Guericke University Magdeburg, FVST/IAUT Environmental Engineering, Universitatplatz 2, Magdeburg 39106, Germany

## ARTICLE INFO

## ABSTRACT

The investigation aims to develop SCR-catalysts with enhanced oxidation activity for elemental mercury. For this, different nano-sized TiO$_2$ particles were coated with 1 and 2 wt.% gold. Suspensions obtained from these particles were used for dip-coating the commercial honeycomb-shaped V$_2$O$_5$–WO$_3$/TiO$_2$ reference SCR catalyst. The mercury oxidation activities of the Au/TiO$_2$-coated catalysts were investigated in the laboratory for the temperature range 180–390 °C and simulated coal-fuel flue gas conditions (O$_2$, SO$_2$, NO, H$_2$O, Hg, HCl and without NH$_3$).

At reaction temperatures from 180 to 320 °C, Au/TiO$_2$ coatings enhanced the mercury oxidation activity of the SCR catalyst significantly by a factor of 2. At higher reaction temperatures the positive effect of the Au/TiO$_2$ coatings on mercury oxidation decreased and was strongly dependent on the HCl content of the flue gas. The impact of Au/TiO$_2$ coatings on the DeNO$_x$ activity of the SCR catalysts at 390 °C was only marginal. The measured SO$_2$/SO$_3$ conversion activity rates depended on the coating procedure and the gold content of the catalysts.

In conclusion, the Au/TiO$_2$ coatings are promising for the development of multi-pollutant SCR-DeNO$_x$ catalysts with high mercury co-oxidation activity for cold-site configurations or flue gases with higher HCl contents.

© 2014 Elsevier B.V. All rights reserved.

## 1. Introduction

Mercury (Hg) is regarded as a hazardous atmospheric pollutant. Once in the atmosphere, elemental mercury (Hg$^{el}$) is subjected to long-distance transport before being oxidised and deposited in water bodies and sediments. In aquatic systems, mercury may be transformed into methyl mercury, a highly toxic compound which bio-accumulates and magnifies once in the food chain. Human health is affected mainly by the consumption of fish contaminated with methyl-Hg [1]. In addition to natural sources, coal-fired power plants, waste incinerators, and cement plants are the major anthropogenic sources of mercury emissions. Due to their persistence, long-range mobility, bio-accumulation in aquatic system and neuro-toxic impact on human health, mercury emission abatement is a new challenge for environmental engineering [2].

### 1.1. Hg emission control

Current models estimate that mercury releases from Europe and the US will decline whereas emissions from the fast growing economies such as India and China will increase [3]. Many countries are regulating mercury emissions. In 2013, the US limited the emissions from coal-fired power plant units in the Mercury and Air Toxic Standards (MATS) [4] resulting in maximum emission concentration for existing plants between 1.4 and 4.1 µg/m$^3$ (STP, dry) at 6 vol.% O$_2$ and as a 30-day average. The Chinese government passed a new emission standard with a maximum mercury emission level of 30 µg/m$^3$ (STP, dry) for thermal power plants [5]. In Germany, a new standard calls for a maximum mercury emissions concentration of 10 µg/m$^3$ (STP, dry) as an annual average for power plants and waste incinerators [6].

* Corresponding author at: Martin-Luther University Halle-Wittenberg, Centre for Engineering Science, D-06099 Halle (Saale), Germany.
** Corresponding author.
*E-mail addresses:* beatriceandreea@yahoo.com, beatrice.dranga@iw.uni-halle.de (B.-A. Dranga), heinz.koeser@ovgu.de (H. Koeser).

The effectiveness of the technologies implemented for the control of mercury emissions in power plants depends on the nature of the mercury species in the flue gases. Oxidised mercury ($Hg^{ox}$) is highly water soluble compared to elemental mercury ($Hg^{el}$), with only a low solubility in the μg/l range. $Hg^{ox}$ is easily removed as a co-benefit of wet flue gas desulphurisation (WFGD) systems. WFGD systems capture approximately 90% of the $Hg^{ox}$ present in the flue gases. Therefore, one of the main challenges of mercury control strategies in power plants is the efficient conversion of elemental mercury into oxidised mercury.

## 1.2. Selective catalytic reduction (SCR) process

The catalytic oxidation of $Hg^{el}$ can be achieved as a co-benefit of SCR units for nitrogen oxides ($NO_x$) reduction (DeNO$_x$) [7]. $V_2O_5$-based SCR-DeNO$_x$ catalysts have been commercially available since the 1980s, and are the most commonly implemented technology for the reduction of nitrogen oxides ($NO_x$). SCR systems are installed in a power plant:

- Upstream of the air pre-heater (APH) and electrostatic precipitator (ESP) referred to as hot site, high dust ($T$ = 340–430 °C).
- Upstream of the APH and downstream of the ESP referred to as hot site and low dust.
- Downstream of the APH and the ESP referred to as cold site and low dust ($T$ = 160–240 °C).
- Downstream of flue gas desulphurisation (FGD) referred to as tail-end ($T$ = 160–240 °C, in this configuration no co-removal of the oxidised mercury can be achieved).

In flue gases containing $SO_2$ the operation temperature has to be increased to above 340 °C in order to avoid the condensation of ammonium sulphates. In commercial practice in power plants most SCR reactors are hot-side, high dust installations. The SCR technology is based on the reduction of nitrogen oxide (NO) with ammonia ($NH_3$) [8]. In a side reaction, SCR catalysts are known to convert sulphur dioxide ($SO_2$) to sulphur trioxide ($SO_3$). A higher $V_2O_5$ content in the SCR catalyst causes an increase in the conversion of $SO_2$ to the undesirable $SO_3$ [9]. The vanadium content of hot-side SCR catalysts is often limited to about 0.5 % in order to suppress this reaction as far as possible.

## 1.3. Hg co-oxidation in SCR-DeNO$_x$ plants

Another co-benefit of SCR catalysts is their oxidation activity for elemental mercury ($Hg^{el}$) [10–15]. This oxidation activity depends on the presence of hydrogen halides (HCl and HBr) in the flue gas [16]. Negligible oxidation occurs when HCl is absent; in this case $Hg^{el}$ is mostly adsorbed by the catalysts [17,18]. The overall oxidation reaction can be summarised as in Eq. (1):

$$Hg + 2HCl + 0.5O_2 \rightarrow HgCl_2 + H_2O \tag{1}$$
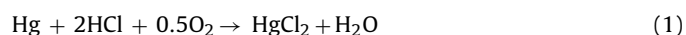
The mercury oxidation activity of SCR catalysts increases with their $V_2O_5$ content and the amount of hydrogen halides in the flue gas to be treated [19,20]. Ammonia, to a certain degree, and in a very pronounced manner the simultaneous presence of $NH_3$ and NO, will cause reduced mercury oxidation activity of SCR-DeNO$_x$ catalysts [19,21]. Due to these inhibitive effects, mercury oxidation takes place mostly at the outlet of an SCR reactor after most of $NH_3$ has been used up in the DeNO$_x$ reaction [7,22].

Even though the commercially available SCR catalysts exhibit a certain degree of mercury oxidation activity, there is a need for more active oxidation catalysts especially for flue gases with low HCl concentration from low chlorine coals. Gold (Au)-based catalysts are likely candidates [7].

## 1.4. Au as an Hg sorbent and Hg oxidation catalyst

Gold has the ability to adsorb mercury on its surface to form an alloy called amalgam. This property has been exploited for decades in analytical chemistry [23] and in gold mining. More recently, Au-coated fixed structures were investigated in demonstration plants for the adsorption and capture of mercury from flue gases for mercury control as part of the MerCAP project [24].

Gold-based catalysts were shown to be active in a large number of oxidation reactions [25]. More recently, gold-based catalysts have also attracted interest from academia and industry for their potential as $Hg^{el}$ oxidation catalysts [26–28]. In addition to adsorbing Hg from gases, gold also has the ability to adsorb species like $Cl_2$ and HCl on its surface. Adsorbed $Cl_2$ molecules are dissociated to chlorine atoms [26] which further react with the adsorbed mercury. The critical importance of the adsorption of HCl on gold was supported by the observation of [29] that when HCl was removed from gas stream, $Hg^{el}$ oxidation continued but with a considerable decrease. Gold exhibits a certain degree of inertness to other flue gas components ($SO_2$, $H_2O$, NO, organic compounds). Experimental investigations showed that these species did not limit $Hg^{el}$ oxidation [26,28].

Over the past decade, pilot [27], and full-scale [30,31] investigations have been conducted with the aim of assessing the $Hg^{el}$ oxidation activity and long-term stability of several honeycomb catalysts including a commercial Au/γ-Al$_2$O$_3$ catalyst under the cold-site low dust conditions of coal-fired power plants. The in-plant demonstration at a temperature of 180 °C and over 17 months of operation showed only a moderate decrease in mercury oxidation activity of the catalyst.

All of the available studies on the mercury oxidation activity of gold-based catalysts have been conducted under cold-site conditions up to temperatures of 225 °C. To date, there is a lack of knowledge about the hot site mercury oxidation activity of Au-based catalysts. In comparison to other noble metals like platinum there are no indications in the literature, that gold is affecting the $SO_2$ to $SO_3$ oxidation reaction appreciably. This was another reason why gold was selected for this investigation.

## 1.5. Scope of the present investigation

The research presented in this paper focuses on efforts to improve the co-oxidation of mercury on SCR-DeNO$_x$ catalysts. For this purpose, a commercial SCR-DeNO$_x$ catalyst was dip-coated with a nano-structured $TiO_2$ layer containing finely dispersed gold particles. The research is to be seen as part of an ongoing research endeavour to develop SCR units into multi-pollutant control devices in power plants.

The mercury oxidation activities of the different catalysts prepared were studied in a laboratory-scale reactor under simulated flue gases typical for coal-fired power plants. $NH_3$ was omitted in order to concentrate on application at the tail-end of SCR-DeNO$_x$ reactors or downstream of the APH. The temperature range studied covered consequently the hot-site and cold-site of power plants.

A commercial hot-site honeycomb-shaped $V_2O_5$–$WO_3$/$TiO_2$ was used as reference catalyst. The mercury oxidation is known to be a fast reaction similar to the DeNO$_x$ reaction occurring near to the surface of the catalyst [19]. Therefore a catalytic active component added is most efficient if located near to the surface. For this, nano-structured coatings of Au/$TiO_2$ were applied to the reference catalysts surface by different methods. The cost of gold was a factor motivating this choice of coating.

The investigation focused on the mercury oxidation activity but the DeNO$_x$ and the $SO_2$/$SO_3$ conversion activities were also selectively studied in order to demonstrate how the gold coatings affected these "standard" properties of a SCR-DeNO$_x$ catalyst. The

tests were performed with small honeycombed-shaped catalyst samples in order to simulate the flow and mass transfer properties as they occur in commercial plants.

## 2. Experimental

This study relates to the preparation and determination of the mercury oxidation, $SO_2/SO_3$ conversion and $DeNO_x$ activities of $SCR-DeNO_x$ catalysts coated with nano-gold–titanium dioxide layers. The flue gas composition was chosen on the basis of conditions in hard coal-fired power plants. The influence of HCl content, temperature and gold loading on mercury oxidation reaction was studied in greater detail.

### 2.1. Catalyst preparation and characterisation

#### 2.1.1. Preparation of type I Au/TiO₂ coating suspension

The preparation of $Au/TiO_2$-coated SCR monolithic catalysts involved two main steps. Firstly, $Au/TiO_2$ powdered catalysts with 1 and 2 wt.% Au were prepared by deposition-precipitation method as described elsewhere [32,33]. Two different commercially available $TiO_2$ powders were employed as supports ($TiO_2$ P25, a mixture of 75% anatase and 25% rutile, and primary particle size of 21 nm from Evonik-Degussa, Germany and $TiO_2$ Hombikat UV100 with 100% anatase, primary particle size <10 nm from Sachtleben, Germany, see also [34]). During maturation at 70 °C and pH ≥ 7, all $Au^{3+}$ complexes found in the solution become strongly attached to the $TiO_2$ particle surface [35]. Afterwards, the catalysts were dried overnight at 100 °C and calcined at 400 °C in airflow for 4 h. Following calcination, the non-crystalline $Au^{3+}$ on $TiO_2$ surface was reduced to metallic $Au^0$ nano-particles. The calcined catalyst powders were further employed for the preparation of stable suspensions. To this end, a calculated amount of $Au/TiO_2$ powder equivalent to a 2 wt.% solid content was dispersed in an $NH_4Cl$ 5 mM solution, ultrasonicated for 5 min and stabilised by the addition of 0.35 wt.% $NH_4$-polyacrylate (Dolapix PC 21, from Zschimmer & Schwarz, Germany). The measured average particle size distribution by volume for type I suspensions varied between 460 nm for 1 wt.% $Au/TiO_2$ P25 and 735 nm for 1 wt.% $Au/TiO_2$ UV100.

#### 2.1.2. Preparation of Au/TiO₂ coating suspension of type II

As an alternative to the type of suspensions prepared as described above, an $Au/TiO_2$ suspension was obtained by dissolving a calculated amount of $HAuCl_4·3H_2O$ in deionised water to obtain 1 and 2 wt.% Au in the $Au/TiO_2$ final catalyst and adjusting the pH to 7–8 by the addition of 0.1 M $NH_4OH$. The solution was heated to 70 °C and the pH value controlled and kept to 7–8. Afterwards, a calculated amount (equivalent to 2 wt.% solid content) of $TiO_2$ support in the form of a stable commercial Aerodisp W 740 X (Evonik-Degussa, Germany) suspension with 40 wt.% solid content was added and kept under continuous stirring for 1 h at 70 °C. By employing this method a significant number of steps in the preparation of the suspension were eliminated. This type of suspension consisted of significantly smaller particles with average size distribution by volume of between 14 nm and 150 nm. Preparing $Au/TiO_2$ suspensions by employing this method raised the question of how much gold is actually coated on the $TiO_2$ suspended particles. To this end, the Au content of the liquid phase of a 2 wt.% $Au/TiO_2$ Aerodisp suspension was determined by ICP-MS method. Firstly, the suspension was destabilised by lowering its pH to ~3 by addition of 0.1 M HCl and then the clear liquid phase was separated by filtration. The results showed that half (199 mg/l) of the Au was dissolved in the clear liquid phase and not coated on the $TiO_2$ particles. The calculated initial dissolved concentration of gold in the solution was of 400 mg/l.

**Table 1**
Characteristic parameters and nomenclature of the monolithic catalysts investigated.

| Catalyst | Coating type |
|---|---|
| Uncoated SCR | |
| 2Au/TiP25-SCR | 2 wt.% Au/TiO₂ P25 |
| 1Au/TiP25-SCR | 1 wt.% Au/TiO₂ P25 |
| TiP25-SCR | TiO₂ P25 |
| 2Au/TiUV100-SCR | 2 wt.% Au/TiO₂ UV100 |
| 1Au/TiUV100-SCR | 1 wt.% Au/TiO₂ UV100 |
| TiUV100-SCR | TiO₂ UV100 |
| 2Au/TiAerod-SCR | 2 wt.% Au/TiO₂ Aerodisp |
| 1Au/TiAerod-SCR | 1 wt.% Au/TiO₂ Aerodisp |
| TiAerod-SCR | TiO₂ Aerodisp |

Pitch: 7.1 mm; wall thickness: 0.87 mm; channel: 6.23 mm.

#### 2.1.3. Coating of reference honeycomb-shaped SCR catalysts

The second step in preparing the $Au/TiO_2$ coated SCR catalysts consisted of dip-coating monolithic commercial reference $SCR-DeNO_x$ catalysts samples (Ceram Porzellanfabrik Frauental, Austria) in the as-prepared suspensions types I and II. Prior to the dip-coating procedure, the SCR monoliths were washed with deionised water in an ultrasonic bath for 15 min and dried overnight. After cooling down, the SCR honeycombs with $2 \times 2$ channels and 10 cm length were immersed for 1 min in the as-prepared suspensions. The excess suspension was removed from the honeycomb surface by holding the sample in a vertical position for 1 min, and then samples were dried at 120 °C overnight and calcined in airflow at 400 °C for 4 h. The SCR monolith samples were weighed before and after the dip-coating procedure with the aim of determining the amount of $Au/TiO_2$ coated on their surface as follows: $m_{coating} = m_{coated\_SCR} - m_{uncoated\_SCR}$. Knowing the mass of $Au/TiO_2$ coatings and the geometrical surface of the SCR samples made it possible to calculate the specific geometrical surface coverage (in μg $Au/TiO_2$ per $mm^2$ of SCR surface).

#### 2.1.4. Characterisation of Au/TiO₂ coated SCR catalyst

The characteristic parameters and nomenclature of the catalyst investigated in this study are given in Table 1. The particle size distributions by volume and intensity in the suspensions were measured by employing the Zetamaster S system from Malvern Instruments (Germany) and a dynamic light scattering system (DLS) HPPS-ET, Malvern Instruments (Germany). Suspension viscosities were determined by employing the AR 2000 system from TA Instruments (USA). BET surface area, pore volume and pore diameter of the SCR monolithic substrate were determined by nitrogen adsorption–desorption on a TriStar II 3020 system (Micromeritics Instruments, USA), while its surface and bulk composition were studied by X-ray fluorescence method by employing the Axios 1 kW system (PANalytical, USA). The XRF composition results are given in Table 2, while the textural properties of uncoated and $Au/TiO_2$-coated SCR catalysts are presented in Table 3. The uncoated and $Au/TiO_2$-coated SCR monoliths surface was studied by means of scanning electron microscopy (SEM) by employing the Hitachi S-4800 system (Japan).

### 2.2. Experimental set-up and procedure

#### 2.2.1. Hg-oxidation activity tests

The $Hg^{el}$ oxidation efficiency of uncoated and $Au/TiO_2$-coated SCR catalysts was investigated on a laboratory scale by employing the experimental set-up given in Fig. 1. It consists of three units: model gas generation, reactor and gas analysis system. A detailed description of the model gas generation unit and the reactor were given in [17]. The honeycomb-shaped catalyst samples with $2 \times 2$ channels and length of approximately 10 cm were placed in a glass reactor consisting of two concentric tubes as described in [17]. Prior

**Table 2**
Surface and bulk composition of the uncoated SCR-DeNO$_x$ honeycomb substrate.

| | Composition (by XRF analysis) (%) | | | | | | | | | |
|---|---|---|---|---|---|---|---|---|---|---|
| | TiO$_2$ | SiO$_2$ | Al$_2$O$_3$ | V$_2$O$_5$ | WO$_3$ | CaO | MgO | Fe$_2$O$_3$ | SO$_3$ | Others[a] |
| Surface | 78.2 | 8.71 | 2.17 | 0.61 | 5.99 | 1.7 | 0.23 | 0.36 | 1.69 | 0.34 |
| Bulk | 77.7 | 8.04 | 2.59 | 0.61 | 5.76 | 2.4 | 0.46 | 0.38 | 1.83 | 0.23 |

[a] Na$_2$O; K$_2$O; P$_2$O$_5$; As.

**Table 3**
Textural properties of uncoated SCR-DeNO$_x$ and of Au/Aerodisp-coated SCR-DeNO$_x$ catalyst samples.

| Catalyst type | BET surface (m$^2$/g) | Pore volume (cm$^3$/g) | Pore diameter (nm) |
|---|---|---|---|
| SCR uncoated | 61.5 ± 0.53 | 0.22 | 13.14 |
| TiAerod/SCR | 69.9 ± 0.15 | 0.23 | 13.34 |
| 2Au/Aerod/SCR | 63.21 ± 0.40 | 0.23 | 14.63 |

to inserting the catalyst test element in the reactor, its outer part was isolated with glass wool, ensuring that the simulated gas would only flow through the inner channels. The catalyst length and gas flow were adjusted to simulate flow conditions and residence time characteristics to one layer of catalyst in an industrial SCR-DeNO$_x$ reactor. For this purpose, an area velocity (AV) of approximately 21 m/h was selected and, linear velocity of 0.36 m/s.

The catalytic investigations were conducted under the standard conditions summarised in Table 4. Carbon dioxide was omitted in the simulated flue gas, because in previous investigations it was shown to have only a negligible effect on mercury oxidation [19]. Prior to the catalytic tests, the samples were aged for one week and, then conditioned under simulated flue gas conditions characteristic for each type of reaction (see Table 4) for 24 h for Hg oxidation and DeNO$_x$ catalytic reactions and 48–72 h for SO$_2$/SO$_3$ conversion tests. When changing experimental parameters (temperature and/or HCl concentration), catalyst samples were left for more than 2 h under the new conditions prior to mercury measurement in order to ensure that stationary conditions for mercury concentration downstream of the catalyst were achieved.

### 2.2.2. Mercury analysis

In order to determine the mercury oxidation activity of the catalysts, the dry mercury sorbent-trap method was employed [36].

For this purpose, the gaseous mercury was sampled before the inlet and at the outlet of the reactor. The mercury gas sampling trains consist of two Dowex/active carbon traps placed in parallel and heated at 80 °C followed by pumps and gas counters. The sorbent traps are connected to the experimental set-up by heating tubes kept at 180 °C to avoid oxidised mercury deposits. In the sorbent traps, a layer of Dowex$^{TM}$ 1 × 8 (mesh size 100 μm, Carl Roth) was followed by a layer of iodised activated carbon (AC) pellets (Carl Roth). The oxidised Hg was selectively adsorbed by the Dowex layer while the elemental Hg was retained in the activated carbon layer. For each reaction parameter, three gaseous mercury samplings were taken with sampling time of 40 min. For each sampling, two Dowex/AC sorbent traps were placed in parallel for reasons of reproducibility. Table 5 shows an example of the variability of the Hg$^{el}$ oxidation efficiency data obtained by employing the Dowex/AC sorbent traps method. The mercury content of the Dowex and activated carbon layers was determined by employing the pyrolytic spectrometer system RA-915/Pyro-915+ from Lumex-Instruments (calibrated with commercial mercury standard solutions), and the data obtained were used to calculate the mercury oxidation activity ($k_{Hg^{el}/Hg^{ox}}$) according to first order principles by employing equation (2):

$$k_{Hg^{el}/Hg^{ox}} = -AV \cdot \ln\left(\frac{1-\eta_{Out}}{1-\eta_{In}}\right), \text{ m/h} \qquad (2)$$

where $k_{Hg^{el}/Hg^{ox}}$ is the mercury oxidation activity in a given flue gas (m/h), AV is the area velocity (m/h), $\eta_{Out} = (Hg^{ox}_{Dowex,Out})/(Hg^{el}_{AC,Out} + Hg^{ox}_{Dowex,Out})$ is the mercury oxidation efficiency measured after the catalyst layer, $\eta_{In} = (Hg^{ox}_{Dowex,In})/(Hg^{el}_{AC,In} + Hg^{ox}_{Dowex,In})$ is the mercury oxidation efficiency measured before the catalyst layer (by-pass values), $Hg^{ox}_{Dowex}$ is the concentration of oxidised mercury measured in the Dowex layer (μg/m$^3$(STP, dry)), $Hg^{el}_{AC}$ is the concentration of
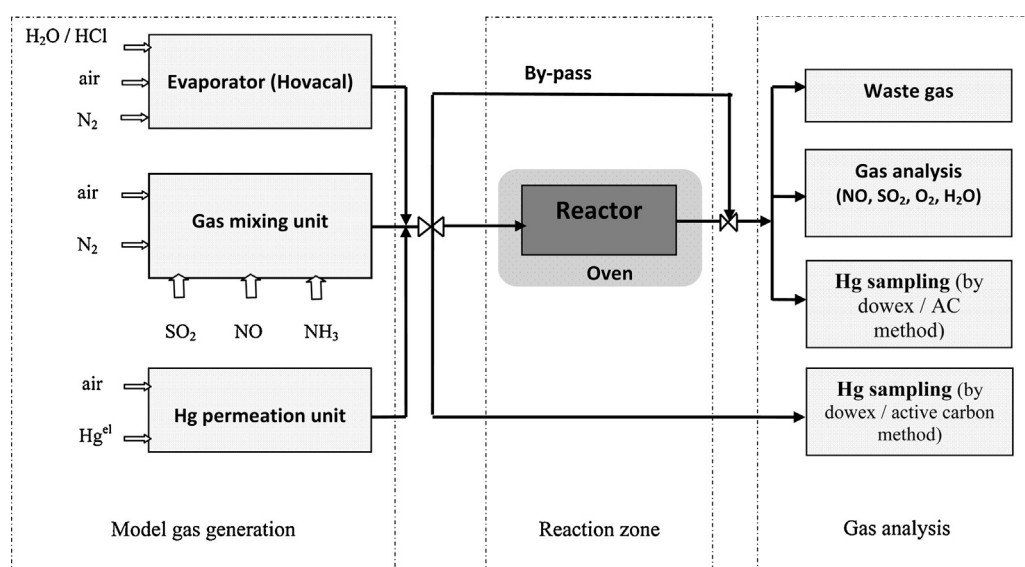


**Fig. 1.** Schematics of the experimental set up for Hg$^{el}$ oxidation tests.

**Table 4**
Experimental flue gas conditions for the catalytic tests.

| | $T$ (°C) | $O_2$ (vol.%, dry) | $H_2O$ (vol.%, wet) | $Hg^{el}$ (µg/m³ STP, dry) | $SO_2$ (ppm, dry) | NO (ppm, dry) | $NH_3$ (ppm, dry) | HCl (mg/m³, STP, wet) | AV (m/h) |
|---|---|---|---|---|---|---|---|---|---|
| Hg oxidation | 180–390 | 4 | 7 | 60–130 | 700 | 400 | – | 10–100 | ~21 |
| DeNO$_x$ | 390 | 4 | 7 | – | 700 | 400 | 400-480 | – | ~21 |
| Ageing and SO$_2$/SO$_3$ conversion | 390 | 4 | 7 | – | 600 | 400 | – | – | ~21 |

$V^0_{g,\,dry}$ : 200 l/h; $V^0_{g,\,wet}$ : 215 l/h.

elemental mercury measured in the AC layer (µg/m³(STP, dry)). The mercury measurements conducted in by-pass showed that approximately 5% of the inflow mercury is already in oxidised form. This result is in line with the empty reactor tests (no catalyst present) where 5.3% of the total mercury was in oxidised state. Because of the oxidised mercury in the inlet gas the equation for calculation of the oxidation activity (2) had a bit unusual form compared to the one used elsewhere in the literature [19].

The non-mercury gas components $H_2O$, $SO_2$ and NO were continuously measured using a multi component BINOS analysis system from Emerson Process (formerly Leybold-Heraeus GmbH) equipped with a hot (200 °C) photometric cell. A paramagnetic OXYNOS analyser was employed for measuring the $O_2$ concentration. All of these devices were regularly calibrated with conventional certified reference gases.

### 2.2.3. SO$_2$-conversion activity tests

SO$_2$/SO$_3$ conversion tests were performed with the aim of determining the amount of SO$_3$ produced over the as-prepared catalysts. In this case an experimental set-up similar to the one in Fig. 1 was used. The test concentrations are given in Table 4. An infrared analyser, HT-Binos 1001 (Rosemount, Germany) was used to measure the SO$_2$ concentration of the model flue gas. SO$_2$ ($C_{SO_2}$) and SO$_3$ ($C_{SO_3}$) concentrations in the simulated flue gas were measured downstream of the catalyst in accordance with VDI methods number 2462 [37,38]. The SO$_3$ concentration was determined by controlled condensation of sulphuric acid aerosols in a glass condenser at 85 °C. This temperature was above water dew point to avoid water condensation in the simulated flue gas, but below sulphuric acid dew point allowing SO$_3$ to be condensed as sulphuric acid aerosols. SO$_2$/SO$_3$ conversion rate ($K_{SO_2/SO_3}$) was calculated according to Eq. (3):

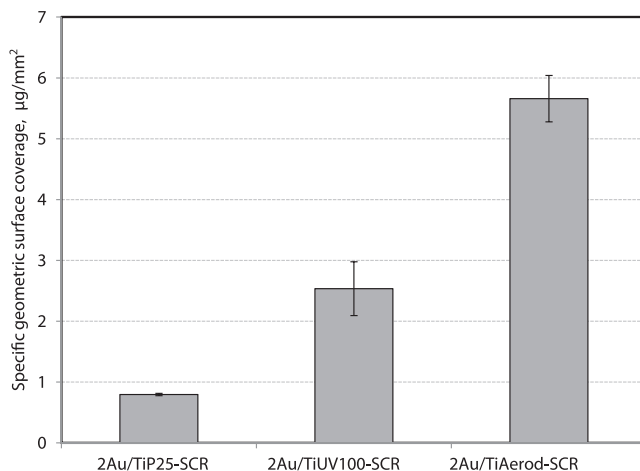$$K_{SO_2/SO_3} = \frac{C_{SO_3}\,(ppm)}{(C_{SO_2}\,(ppm) + C_{SO_3}\,(ppm))} \times 100\,(\%) \qquad (3)$$

### 2.2.4. NO$_x$ activity tests

DeNO$_x$ activity of uncoated and Au/TiO$_2$-coated SCR catalysts was determined at a temperature of 390 °C and NH$_3$/NO molar ratios of 1 and 1.2 by employing the experimental set-up shown



**Fig. 2.** Specific geometric surface coverage of SCR-DeNO$_x$ substrates with Au/TiO$_2$ layers in µg Au/TiO$_2$ per mm² SCR.

in Fig. 1. DeNO$_x$ activity was calculated according to the first order reaction equation.

## 3. Results and discussion

### 3.1. Catalysts preparation and characterisation

The Au/TiO$_2$ suspensions employed exhibited similar rheological properties, with viscosities comprised between 1.61 and 1.72 mPa s. The particles size distribution in the as-prepared suspensions varied widely. The 1 wt.% Au/Aerodisp (type II) suspension showed the lowest mean particle size distribution by intensity of 13 nm, while for the 2 wt.% Au/TiO$_2$ P25 suspension (type I) the highest mean particle size distribution was 2360 nm.

Fig. 2 depicts the calculated specific geometrical surface coverage for three different coated catalysts. By employing the type II suspension of Au/Aerodisp for coating, a high surface coverage of 5.7 µg Au/TiO$_2$ per mm² of SCR surface was achieved. The type I suspension of Au/TiO$_2$ P25 led to a much lower coverage of 0.8 µg/mm².

**Table 5**
Example of results reproducibility for Hg$^{el}$ oxidation efficiency (%) data obtained by employing Dowex/AC sorbent traps method and total Hg mass balance.

| 2Au/TiUV100-SCR (sample I) | | | | | 2Au/TiUV100-SCR (sample II) | | |
|---|---|---|---|---|---|---|---|
| | | | Hg$^{tot}_{in}$ (µg/m³,STP dry) | Hg$^{tot}_{out}$ (µg/m³, STP dry) | | | |
| Hg sampling 1 (40 min) | Sorbent trap A | 92.2% | 96.6 | 98.6 | Hg sampling 1 (40 min) | Sorbent trap A | 92.1% |
| | Sorbent trap B | 91.7% | | 87.5 | | Sorbent trap B | 93.3% |
| Hg sampling 2 (40 min) | Sorbent trap A | 91.0% | 90.4 | 91 | Hg sampling 2 (40 min) | Sorbent trap A | 91.9% |
| | Sorbent trap B | 91.0% | | 90 | | Sorbent trap B | 92.3% |
| Hg sampling 3 (40 min) | Sorbent trap A | 91.6% | 89.9 | 89.5 | Hg sampling 3 (40 min) | Sorbent trap A | 94.5% |
| | Sorbent trap B | 92.1% | | 87.6 | | Sorbent trap B | 92.3% |
| Average | | 91.6% ± 0.52 | 92.3 ± 3.7 | 90.7 ± 4.1 | Average oxidation (%) | | 92.7% ± 0.99 |

Sorbent traps A and B were placed in parallel; Hg$^{el}$ efficiency (%) = Hg$^{ox}_{Dowex}$/(Hg$^{ox}_{Dowex}$ + Hg$^{el}_{AC}$) × 100; reaction temperature 320 °C and 100 mg/m³ HCl, variability given as standard deviation (±), Hg$^{tot}_{in}$ – total Hg measured before the reactor inlet (by-pass), and Hg$^{tot}_{out}$ – total mercury measured at the reactor outlet (after the catalyst).
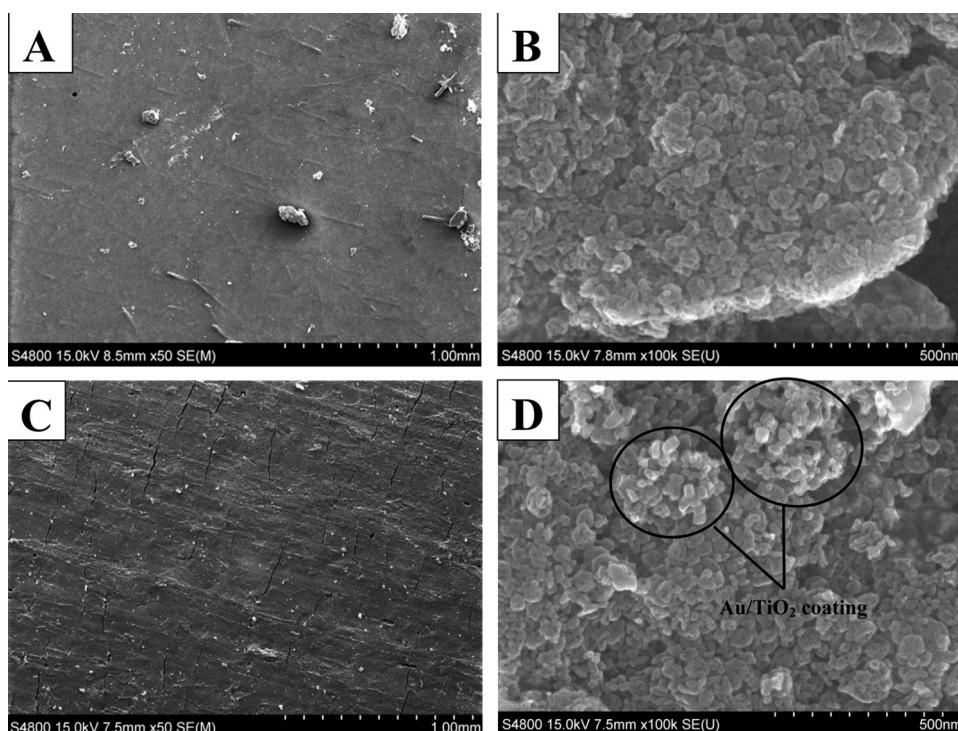
**Fig. 3.** Scanning electron micrographs for: (A and B) uncoated SCR catalyst surface and (C and D) 2Au/TiP25-SCR catalyst surface.

In Fig. 3 SEM micrographs for uncoated SCR and 2Au/TiP25-SCR monolith surfaces are given. As can be seen in Fig. 3A, the uncoated SCR monolith had a relatively smooth surface with a visible porous structure (Fig. 3B). When looking at the coated SCR monolith surface, Fig. 3C, it should be noted that the Au/TiO₂ layers consisted of irregularly shaped agglomerates. Zooming in on one of these agglomerates, Fig. 3D, reveals that the gold-coated TiO₂ particles sized less than 100 nm form a tightly packed, sponge-like structure. A similar morphology was observed for the prepared Au/P25-TiO₂ catalyst powders (SEM micrographs not shown here), where the primary particles also formed tightly packed agglomerates. Images obtained in the backscattering mode of the SEM combined with energy dispersive X-ray (EDX) analysis showed that the coated P25 particles on the surface differed in their gold content.

### 3.2. Hg$^{el}$ oxidation activity

The focus of the experimental investigations was placed on the Hg oxidation activity of gold coating in reference to uncoated SCR-DeNO$_x$ catalysts under simulated flue gas conditions, where the concentration of Hg$^{el}$ varied between 60 and 130 μg/Nm³. Considering that the prepared gold-coated SCR monoliths are intended for use as a final catalyst layer in the SCR reactor, the inhibitory effect of NH₃ on mercury oxidation activity is no longer of great concern here, therefore the effect of NH₃ was not studied. In coal-fired power plants, the hydrogen chloride (HCl) content of the flue gases is primarily determined by the halogen content of the coal and may typically vary between 1 and 500 mg/m³ [39]. Generally, HCl is the dominant form in which chlorine species are found in flue gases. To determine the extent to which HCl influences Hg$^{el}$ oxidation activities of gold coated SCR catalysts, two concentrations of 10 and 100 mg/m³ were selected. The temperatures investigated covered the cold-site to hot-site range from 180 to 390 °C.

### 3.2.1. Effect of different Au/TiO₂ coatings on Hg$^{el}$ oxidation

This part of experimental investigation aims to determine which type of Au/TiO₂ coating has the highest impact on the Hg$^{el}$ oxidation activity of the SCR catalyst selected as a support. The reaction temperatures of 180 and 390 °C and an HCl concentration of 100 mg/m³ were selected. Fig. 4 depicts the Hg$^{el}$ oxidation activities of the uncoated SCR catalyst and those of SCR catalysts covered with different types of coatings containing 2 wt.% Au. Applying Au/TiO₂ coatings to the surface of SCR catalyst resulted in a significant enhancement of Hg$^{el}$ oxidation activity. The most visible influence of Au/TiO₂ coatings on Hg$^{el}$ oxidation activity was observed at 180 °C. At this temperature, the selected SCR-uncoated reference catalyst exhibited a relatively low Hg$^{el}$ oxidation activity, which was expected considering that the selected commercial SCR-DeNO$_x$ catalysts for hot site conditions was designed with a V₂O₅ content below 1%. By applying an Au/TiO₂ coating, the Hg$^{el}$ oxidation activity at 180 °C was boosted from about 18 m/h for the uncoated SCR-catalyst to 38 m/h for the 2Au/TiAerod-SCR catalyst. When increasing the reaction temperature to 390 °C, the uncoated SCR catalyst showed a much higher mercury oxidation activity of 29 m/h. However, although at this high temperature the Hg$^{el}$ oxidation activity increased as a consequence of coating with Au/TiO₂, the effect is significantly lower when compared with that measured at 180 °C.

From these results, it is obvious that the effect of Au/TiO₂ coatings on Hg$^{el}$ oxidation activity is somewhat limited at higher temperatures. The lower performance of Au/TiO₂ coatings at 390 °C may be explained by the decreased Au–Hg adsorption/amalgamation at higher temperatures [40]. The importance of the mercury being adsorbed on the gold surface for the oxidation process has already been pointed out in literature [41].

When it comes to the effect of the different prepared Au/TiO₂ coatings on the oxidation activity, no significant differences were detected.

### 3.2.2. Effect of gold loads on Hg$^{el}$ oxidation activity

Since the previous experimental results show that gold coatings have the highest impact on Hg$^{el}$ oxidation under cold site conditions, it seemed appropriate to select 180 °C temperature to
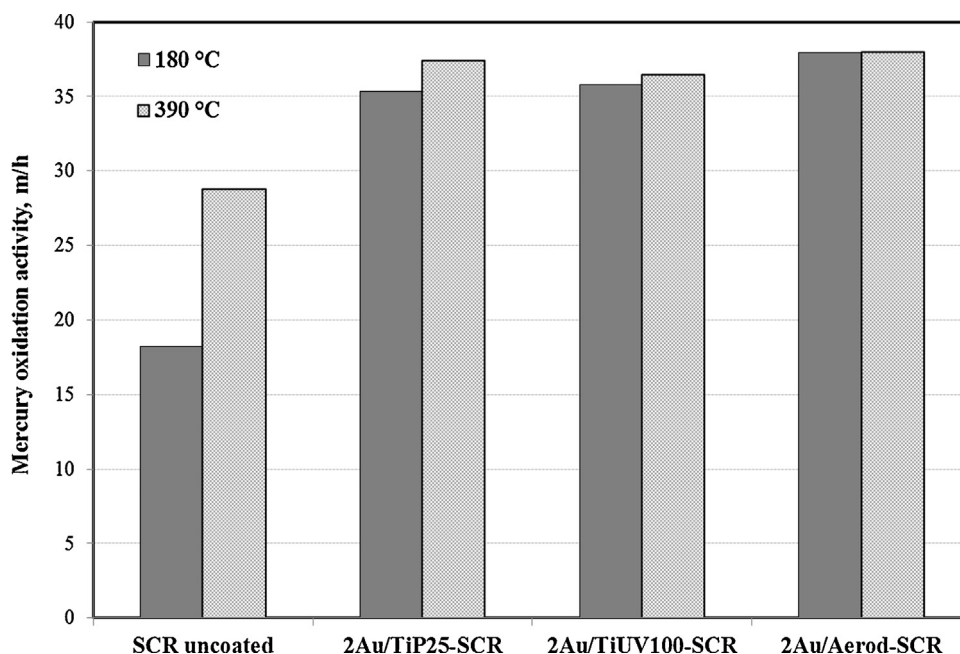
**Fig. 4.** Effect of Au/TiO$_2$ coatings type on Hg$^{el}$ oxidation activity under flue gas conditions given in Table 4 and 100 mg/m$^3$ HCl at 180 and 390 °C.

investigate the effect of gold loads on Hg$^{el}$ oxidation. Table 6 depicts the effect of 1 and 2 wt.% gold on the Hg$^{el}$ oxidation activity of Au/TiO$_2$-coated SCR catalysts. When the HCl concentration of the flue gas is 100 mg/m$^3$, a negligible difference is observed in Hg oxidation activity as a function of gold loads. Similar results were obtained when the HCl concentration was only 10 mg/m$^3$. In all cases the coated catalysts show activity of approximately twice that of the uncoated reference. It appears that the lower gold loads investigated do not cause a significant decrease in Hg$^{el}$ oxidation activity. These findings are encouraging from an economic point of view when considering the cost of gold as a coating material. The study of gold loads on mercury oxidation activity should be carried out further for loads of less than 1 wt.% with the aim of determining an optimum.

### 3.2.3. Effect of reaction temperature and HCl content on Hg$^{el}$ oxidation activity

The mercury oxidation activities were determined under the simulated flue gas conditions given in Table 4 and the temperature range 180–390 °C which is from cold-site to hot-site power plant conditions. The evaluated catalysts cover a wide range of activities from 3 m/h up to 52 m/h, see Fig. 5A and B. These variations in Hg$^{el}$ oxidation activities are due to the type of catalyst, reaction temperature and HCl content of the flue gas. It can be seen that coating the surface of the commercial reference SCR-DeNO$_x$ catalyst with Au/TiO$_2$ led to a significant enhancement of Hg$^{el}$ oxidation activity in the temperature interval 180–320 °C. The oxidation activity of all investigated catalyst samples reached a maximum of around 320 °C irrespective of the HCl content of the flue gas. Further increasing

the temperature up to 390 °C caused the Hg$^{el}$ oxidation activity to decrease. This decrease in the Hg oxidation activity of uncoated SCR catalysts at hot site temperatures was noted by other authors as well [19,42,43]. Studies in literature on a wider temperature range for V$_2$O$_5$–WO$_3$/TiO$_2$ SCR-DeNO$_x$ resulted in a maximum activity between 300 and 400 °C [14], whereas a CeO$_2$/TiO$_2$ catalyst showed a maximum of around 250 °C [44]. From this it appears that the decreasing mercury oxidation rate of commercial SCR-DeNO$_x$ catalysts at the high temperatures on the operation side seems to be a common feature of the system.

When analysing the results of Hg$^{el}$ oxidation activities for an HCl concentration of 10 mg/m$^3$ (Fig. 5B), a few surprising findings can be outlined. Firstly, in the temperature interval 180–320 °C, Hg$^{el}$ oxidation activities were relatively close when HCl concentrations were 100 mg/m$^3$. After increasing the temperature further, a decrease in Hg$^{el}$ oxidation activity is observed for all types of catalysts investigated in flue gases with 100 as well as 10 mg/m$^3$ HCl. However, this drop in activity is much stronger in flue gas with the low HCl content of 10 mg/m$^3$. Here, all of the observed mercury oxidation activities shown in Fig. 5B are below 7 m/h at 390 °C. Similar results were recorded for the 2Au/TiAerod-SCR catalysts (data not shown here).

From Fig. 5B it can be seen that at temperatures higher than around 350 °C gold-coatings of the reference SCR-DeNO$_x$ catalysts no longer improved mercury oxidation appreciably. At these high temperatures and low HCl concentrations in the flue gas, it is possible to conclude that mercury oxidation is caused almost exclusively by the SCR substrate and not appreciably by gold coatings applied to the surface. Obviously the effect of the gold

**Table 6**
Effect of gold loads (1 and 2 wt.% Au) on Hg$^{el}$ oxidation activity over Au/TiO$_2$-coated SCR-DeNO$_x$ monoliths at 180 °C and, 100 and 10 mg/m$^3$ HCl.

| Catalyst type | $k_{Hg}$, m/h (100 mg/m$^3$ HCl) | $k_{Hg\ coated}/k_{Hg\ uncoated}$ (100 mg/m$^3$ HCl) | $k_{Hg}$, m/h (10 mg/m$^3$ HCl) | $k_{Hg\ coated}/k_{Hg\ uncoated}$ (10 mg/m$^3$ HCl) |
|---|---|---|---|---|
| SCR uncoated | 18.2 ± 1.35 | | 16.6 ± 1.92 | |
| 2Au/TiP25-SCR | 35.4 ± 5.28 | 1.95 | 31 ± 1.38 | 1.87 |
| 1Au/TiP25-SCR | 33.4 ± 3.05 | 1.84 | 30.2 ± 2.52 | 1.82 |
| 2Au/TiUV100-SCR | 35.8 ± 1.27 | 1.97 | 33.1 ± 1.05 | 1.99 |
| 1Au/TiUV100-SCR | 35.06 ± 3.18 | 1.93 | 33.6 ± 2.28 | 2.02 |
| 2Au/TiAerod-SCR | 38 ± 1.27 | 2.09 | 38.4 ± 1.84 | 2.31 |
| 1Au/TiAerod-SCR | 40.2 ± 1.27 | 2.21 | 39.8 ± 1.06 | 2.4 |
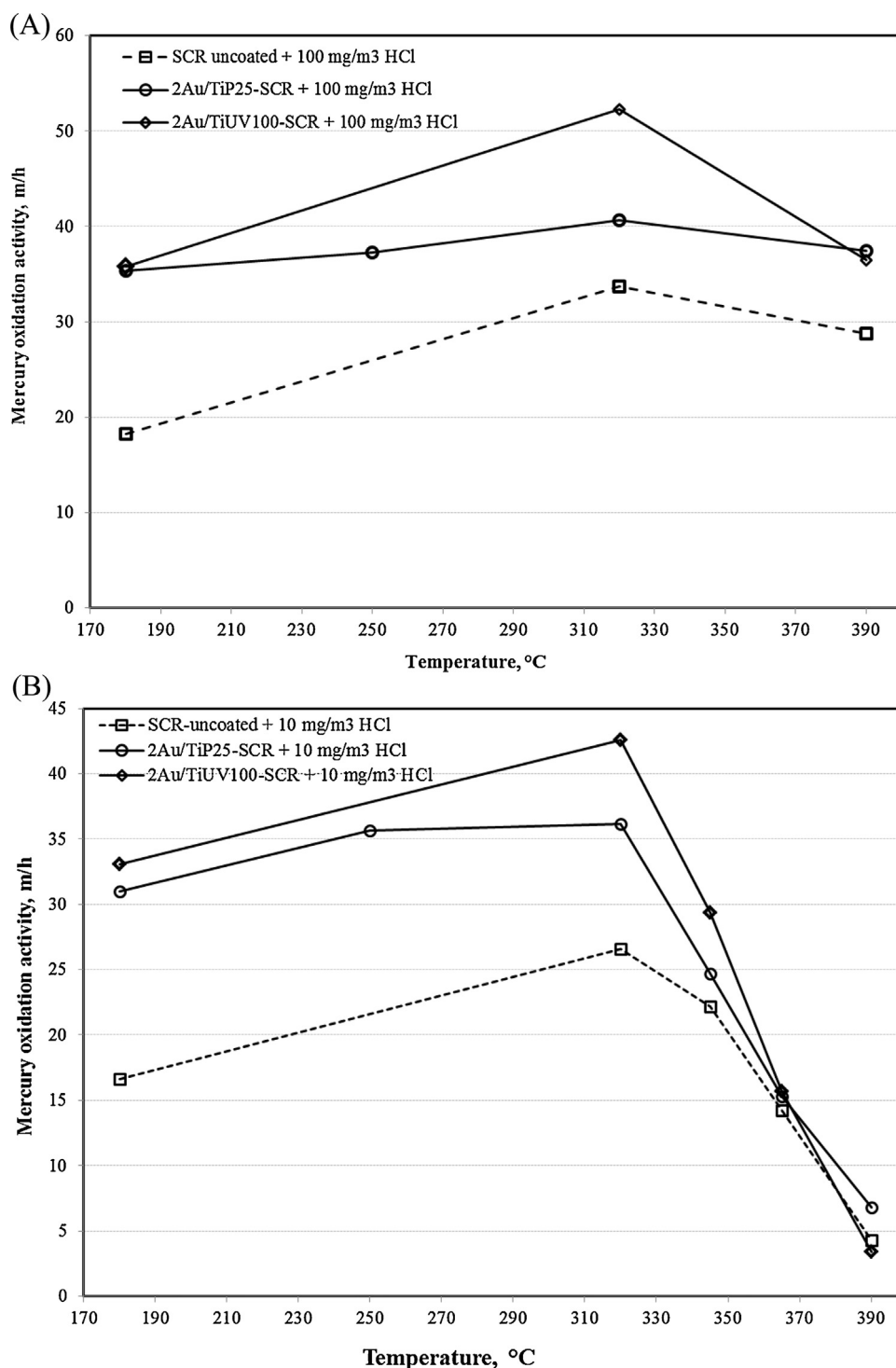
**Fig. 5.** (A) Effect of reaction temperature on Hg$^{el}$ oxidation over uncoated and Au/TiO$_2$-coated SCR-DeNO$_x$ monoliths at 100 mg/m$^3$ HCl in the flue gas. (B) Effect of reaction temperature on Hg$^{el}$ oxidation over uncoated and Au/TiO$_2$-coated SCR-DeNO$_x$ monoliths at 10 mg/m$^3$ HCl in the flue gas.

also depends to a significant extent on the adsorption of a chlorine species on its surface, as has already been predicted by theoretical considerations [45]. Higher temperatures decrease the adsorption and consequently surface concentration of the chlorine species.

### 3.2.4. Possible mechanistic pathways for mercury oxidation on Au/TiO$_2$-coated SCR catalysts

When discussing potential mechanisms for the oxidation of Hg$^{el}$ on the Au/TiO$_2$-coated SCR catalysts surface an important aspect must be taken in account, namely the presence of two different

active sites (Au- and V$_2$O$_5$-active sites) on the catalysts surface. Au and V$_2$O$_5$ active-sites are known to adsorb mercury on their surface [17,29]. Surface experimental studies conducted on the SCR catalysts suggested that V$_2$O$_5$-active sites oxidise elemental mercury via Langmuir–Hinshelwood mechanism with both adsorbed Hg$^{el}$ and HCl species reacting to form weakly adsorbed HgCl$_2$ which is subsequently desorbed from the catalyst surface [7]. Recent density function theory (DFT) modelling study [45] suggests that the Hg$^{el}$ oxidation on Au (111) surfaces in the presence of chlorine species may occur in a step by step process (Hg → HgCl → HgCl$_2$)

**Table 7**

Comparison of $Hg^{el}$ oxidations ($DeNO_x$-inactive) and $DeNO_x$ activities of reference and gold coated SCR monoliths at 390 °C and simulated flue gas composition given in Table 4.

| Catalyst | $k_{Hg}$, m/h (100 mg/m$^3$ HCl) | $k_{Hg}$, m/h (10 mg/m$^3$ HCl) | $k_{DeNO_x}$, m/h (NH$_3$/NO = 1.2) | $k_{DeNO_x}$, m/h (NH$_3$/NO = 1) |
|---|---|---|---|---|
| SCR uncoated | $28.8 \pm 2.4$ | $4.3 \pm 0.58$ | $38.5 \pm 1.0$ | 39 |
| 2Au/TiUV100-SCR | $36.5 \pm 3.05$ | $3.4 \pm 0.35$ | $40.9 \pm 1.52$ | $41.7 \pm 0.1$ |
| 2Au/TiAerod-SCR | $38 \pm 4.58$ | $2.6 \pm 0.53$ | $41.51 \pm 2.0$ | $40.7 \pm 2.35$ |

via a Langmuir–Hinshelwood mechanism where $Hg^{el}$ and $Cl_2$ (or HCl) species are separately adsorbed on the gold surface.

Therefore, we can assume that the elemental mercury oxidation in the presence of HCl on the $Au/TiO_2$-coated SCR catalysts surface occurs most likely via two separate Langmuir–Hinshelwood mechanisms where both $Hg^{el}$ and HCl species from the flue gas are adsorbed in parallel onto the Au and $V_2O_5$-active sites. The adsorbed $Hg^{el}$ and HCl further react to form $HgCl_2$ which is readily desorbed from the catalyst surface.

The temperature dependence of these two reactions is different. It is known that the $V_2O_5$ based mercury oxidation mechanism is inhibited by ammonia and the $DeNO_x$ reaction [19,21]. Nothing so far is known, that the Au might show similar inhibition effects. Further studies are needed to verify this hypothesis.

### 3.3. Effect of Au/TiO_2 coatings on NO_x reduction and SO_2/SO_3 conversion

$NO_x$ reduction tests were performed at 390 °C and in the presence of $NH_3$/NO ratios of 1 and 1.2 respectively. As can be observed in Table 7, the presence of $Au/TiO_2$ coatings on the surface of the SCR-$DeNO_x$ catalyst only caused a slight increase in $DeNO_x$ activity.

In addition to reducing $NO_x$ and oxidising elemental mercury, the SCR catalysts convert $SO_2$ to $SO_3$ in flue gases [46–48]. Compared to the $DeNO_x$ and mercury reactions, which are relatively fast reactions, the $SO_2$/$SO_3$ conversion is a slow chemistry-controlled reaction which takes place within the whole porous catalyst. In practice, the $SO_2$ from flue gas diffuses into the SCR catalyst's porous structure and is oxidised to $SO_3$ in the presence of $O_2$. The presence of sulphur trioxide leads to the formation of undesirable sulphuric acid mist in the flue gas causing corrosion on the plant equipment and plume opacity of power plants.

$SO_3$/$SO_2$ conversion was determined in the absence of $NH_3$ and $Hg^{el}$ from the simulated flue gas and after at least 48 h of catalyst preconditioning. Details of the reaction parameters are given in Table 4. In order to establish the extent to which the presence of gold in the coatings increases the $SO_2$/$SO_3$ conversion rate, all types of catalyst prepared were tested for this reaction. Fig. 6 depicts the $SO_2$/$SO_3$ conversion results. The uncoated SCR catalyst showed a $SO_2$/$SO_3$ conversion rate of 1.72% under the chosen reaction parameters. When looking at the additional experimental results, it can be observed that the presence of $Au/TiO_2$ layers on the SCR monoliths surface led to an increase in $SO_2$/$SO_3$ conversion. Significant increase in conversion of $SO_2$ to $SO_3$ was measured when the gold loads of the coated layers were 2 wt.%, reaching a maximum value of 6.66% for the 2Au/TiAerod-SCR catalyst. It should be noted that the type II dispersion with Aerodisp contains 50% dissolved gold. The dissolved gold will also have coated the inner surface of the porous catalyst, not only the outer surface as the $Au/TiO_2$ particles. $SO_2$/$SO_3$ conversion followed the order: SCR-uncoated < 2Au/TiUV100-SCR < 2Au/TiP25-SCR < 2Au/TiAerod-SCR. By comparison, 1 wt.% Au in the coating led to a significantly lower conversion rate.

The gold-based coatings investigated consist of relatively low amounts of gold whereas the $TiO_2$ substrate is the major component. The question of how much influence is exerted by the $TiO_2$ on $SO_2$/$SO_3$ conversion arises. With this purpose in mind the
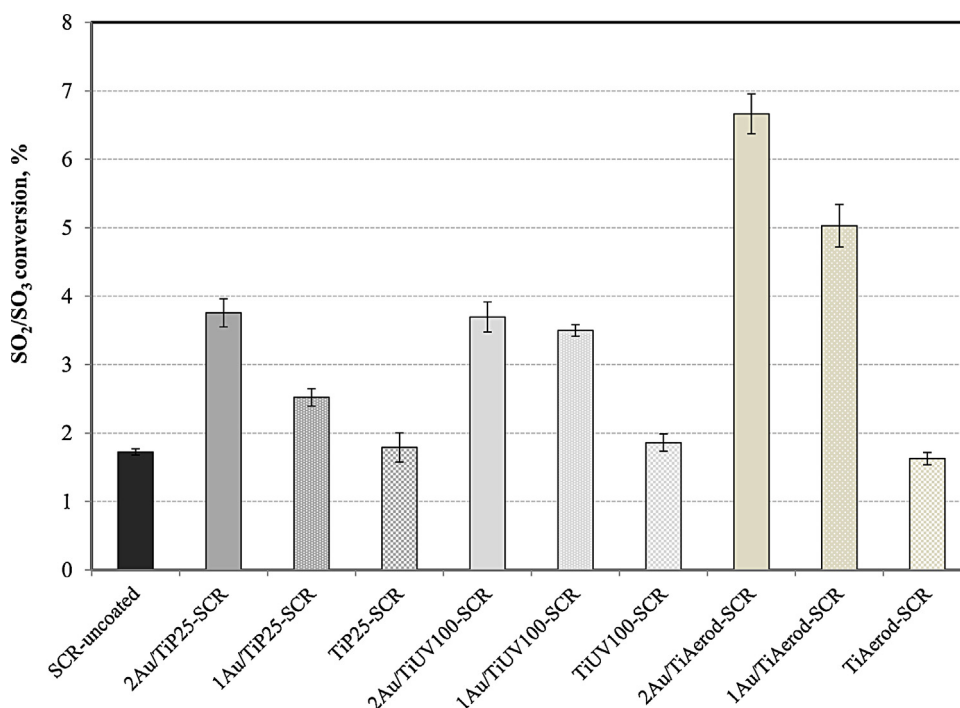


**Fig. 6.** $SO_2$/$SO_3$ conversion of uncoated and gold coated SCR-$DeNO_x$ catalysts at 390 °C.

conversion of $SO_2$ to $SO_3$ for $TiO_2$ coated samples was also investigated. The presence of $TiO_2$ on the surface of SCR catalysts seems to cause a small increase for the SCR samples coated with type I suspensions (TiP25-SCR and TiUV100-SCR) without gold coating and a slight decrease for $TiO_2$ coatings obtained by type II suspension (TiAerod-SCR) (see Fig. 6). These findings seem to indicate that the oxidation activity of the gold mainly affects the $SO_2$ conversion. It should be noted that the $SO_2/SO_3$ conversion rate over SCR catalysts has been shown to be influenced by a number of factors [15,46,47]. A major factor is that a much lower $SO_2/SO_3$ conversion rate is expected once the reaction temperature decreases.

It should be noted that the $NO_x$ reduction and $SO_2/SO_3$ conversion investigations were conducted in the absence of mercury. Mercury will compete with these reactions for the oxygen. From a mass balance point of view this competition (with mercury in the ppb concentration range) will be small. In the presence of HCl there is no appreciable net adsorption of mercury on the catalysts. Therefore it is assumed, that the inhibitory effect of the mercury on the $NO_x$ and $SO_2/SO_3$ reactions should be negligible.

## 4. Conclusions

The investigation has shown that by dip-coating with respective suspensions, $Au/TiO_2$-nano-particles can be applied to the surface of structured SCR-DeNO$_x$ catalysts. This treatment is of interest for manufacturing catalysts but could also be added to the regeneration procedure applied to spent SCR catalysts [49].

Subsequently it was shown in laboratory-scale experiments that $Au/TiO_2$ coatings of a commercial $V_2O_5$–$WO_3$/$TiO_2$ SCR-DeNO$_x$ catalyst improved mercury oxidation capabilities. This enhancement of oxidation activity, however, is dependent on the reaction temperature and the HCl concentration of the flue gas. The maximum mercury oxidation activity of the gold-coated and the reference SCR-DeNO$_x$ substrates is between 300 and 350 °C. It appears that $Au/TiO_2$ coatings are most active in the temperature interval 180–320 °C under cold site conditions in a power plant, with increases in mercury oxidation activity by a factor of 2. Another very interesting finding is that at 180 °C varying the HCl concentration in the flue gas between 10 and 100 mg/m$^3$ and/or gold loads of the coated layers between 1 and 2 wt.% did not lead to significant changes in mercury oxidation activity. A dramatic decrease in oxidation activity was observed once the reaction temperature was increased to above 350 °C and the HCl content was as low as 10 mg/m$^3$.

From the experimental observation it appears that the oxidation of mercury on the surface of the gold is a reaction between adsorbed mercury and adsorbed chlorine species as proposed in the literature [45]. At temperatures below 320 °C, the absorbed HCl-derived species are sufficiently available and do not affect the rate-limiting step. However, at temperatures above 320 °C the adsorption of chlorine will decrease and becomes a rate limiting factor. It should be noted that increasing the operating temperatures to above 400 °C will increasingly shift the thermodynamic equilibrium from the oxidised to the elemental mercury. These findings with respect to the temperature and HCl dependence should also be of importance for the refinement of kinetic models of mercury co-oxidation on SCR catalysts, although this was not the focus of this study.

Another important aspect of this investigation was that the $NO_x$ activity of the as-prepared catalysts was only slightly changed by the applied $Au/TiO_2$ coatings, at least under hot-site conditions of 390 °C. The conversion of $SO_2/SO_3$ over SCR catalysts also has a major impact on the catalyst design and use in industrial SCR units. The reference SCR catalyst converted $SO_2$ to $SO_3$ to a certain degree at 390 °C, but its conversion activity was increased by

coating with $Au/TiO_2$. Results clearly showed that at 390 °C, the Au on the SCR catalysts surface was responsible for the increase in $SO_2/SO_3$ conversion. This increase varied with the Au load and coating type.

Further investigations should address the possible mechanistic pathways of mercury oxidation over the $Au/TiO_2$-coated SCR catalysts in more detail. The most interesting aspect of further studies will the verification of the hypothesis that mercury oxidation on Au based catalyst is not inhibited by ammonia and the DeNO$_x$ reaction. The other aspect of interest is the study of the influence of the possible impact of gold coatings on the conversion of NO to $NO_2$. The stability of the surface $Au/TiO_2$ coatings under power plant conditions also warrants further detailed consideration.

## Acknowledgements

## References

[1] M. Karagas, A.L. Choi, E. Oken, M. Horvat, R. Schoeny, E. Kamai, Environ. Health Perspect. 120 (6) (2012) 799–806.
[2] Division of Technology, Industry and Economics (DTIE) Chemicals Branch, Study on Mercury Sources and Emissions and Analysis of the Cost and Effectiveness of Control Measures, UNEP, Geneva, Switzerland, 2010.
[3] P. Rafaj, I. Bertok, J. Cofala, W. Schöpp, Atmos. Environ. 79 (2013) 472–479.
[4] US EPA Federal Register, Mercury and Air Toxic Standards (MATS) 78, 2013, pp. 24073–24094.
[5] M.E.P.C., A.Q.S.I.Q., Emission Standard of Air Pollutants for Thermal Power Plants, GB 13223-2011, China Environmental Science Press, Beijing, 2011.
[6] 13th BImSchV, Federal Immission Control Ordinance for Large Combustion Plants, and 17th BImSchV Federal Immission Control Ordinance on Waste Incineration and Co-incineration Facilities, Berlin, 2013.
[7] B.A. Dranga, L. Lazar, H. Koeser, Catalysts 2 (2012) 139–170.
[8] J. Svachula, N. Ferlazzo, P. Forzatti, E. Tronconi, F. Bregani, Ind. Eng. Chem. Res. 32 (6) (1993) 1053–1060.
[9] P. Forzatti, I. Nova, A. Beretta, Catal. Today 56 (4) (2000) 431–441.
[10] S. Niksa, N. Fujiwara, J. Air Waste Manage. Assoc. 55 (12) (2005) 1866–1875.
[11] C.L. Senior, J. Air Waste Manage. Assoc. 56 (1) (2006) 23–31.
[12] Y. Eom, S.H. Jeon, T.A. Ngo, J. Kim, T.G. Lee, Catal. Lett. 121 (3–4) (2008) 219–225.
[13] S. He, J. Zhou, Y. Zhu, Z. Luo, M. Ni, K. Cen, Energy Fuels 23 (1) (2008) 253–259.
[14] W. Gao, Q. Liu, C.Y. Wu, H. Li, Y. Li, J. Yang, G. Wu, Chem. Eng. J. 220 (2013) 53–60.
[15] T. Schwämmle, F. Bertsche, A. Hartung, J. Brandstein, B. Heidel, G. Scheffknecht, Chem. Eng. J. 222 (2013) 274–281.
[16] B.W. Vosteen, R. Kanefke, H. Koeser, VGB Powertech 86 (3) (2006) 70–75.
[17] S. Straube, T. Hahn, H. Koeser, Appl. Catal. B: Environ. 79 (2008) 286–295.
[18] S. Eswaran, H.G. Stenger, Energy Fuels 19 (2005) 2328–2334.
[19] R. Stolle, H. Koeser, H. Gutberlet, Appl. Catal. B: Environ. 144 (2014) 486–497.
[20] Y. Zhuang, J. Laumb, R. Liggett, M. Holmes, J. Pavlish, Fuel Process. Technol. 88 (2007) 929–934.
[21] K. Madsen, Mercury Oxidation over Selective Catalytic Reduction (SCR) Catalysts (Thesis), Technical University of Denmark (DTU), 2011.
[22] M. Rallo, B. Heidel, K. Brechtel, M.M. Maroto-Valer, Chem. Eng. J. 198 (2012) 87–94.
[23] J. Lusilao-Makiese, E. Tessier, D. Amouroux, E. Cukrowska, Int. J. Anal. Chem. (2014) 1–8.
[24] J.H. Pavlish, L.L. Hemre, Y. Zhuang, Fuel 89 (4) (2010) 838–847.
[25] G.C. Bond, C. Louis, D.T. Thompson, Catalysis by Gold, Imperial College Press, London, UK, 2006.
[26] Y. Zhao, M.D. Mann, J.H. Pavlish, B.A.F. Mibeck, E.G. Dunham, E.S. Olson, Environ. Sci. Technol. 40 (2006) 1603–1608.
[27] G. Blythe, T. Machalek, B. Lani, R. Rhudy, B. Wiemuth, J. Kyle, D.S. Bishop, URS Power, Technical Paper 50, 2010, pp. 1–11.
[28] J.A. Hrdlicka, W.S. Seames, M.D. Mann, D.S. Muggli, C.A. Horabik, Environ. Sci. Technol. 42 (2008) 6677–6682.
[29] A.A. Presto, E.J. Granite, Platin. Met. Rev. 52 (2008) 144–154.
[30] G. Blythe, C. Miller, B. Freeman, J. Madrid, Full-scale demonstration of oxidation catalyst for enhanced mercury control by wet FGD, in: Proceedings of Power Plant Air Pollutant Control Mega Symposium, Baltimore, MD, USA, August, 2008.

[31] M.G. Blythe, J. Paradis, Full-Scale Testing of a Mercury Oxidation Catalyst Upstream of a Wet FGD System, Final Technical Report; Cooperative Agreement No. DE-FC2606NT42778, DOE-NETL, Austin, TX, USA, 2010.

[32] M. Haruta, T. Kobayashi, H. Sano, N. Yamada, Chem. Lett. 2 (1987) 405–408.

[33] M.A. Centeno, M.C. Hidalgo, M.I. Dominguez, J.A. Navio, J.A. Odriozola, Catal. Lett. 123 (2008) 198–206.

[34] M. Mehrvar, W.A. Anderson, M. Moo-Young, Int. J. Photoenergy 4 (4) (2002) 141–146.

[35] S. Oros-Ruiz, R. Zanella, R. Lopez, A. Hernandez-Gordillo, R. Gomez, J. Hazard. Mater. 263P (2013) 2–10.

[36] J. Mayer, S. Hopf, F. Van Dijen, A. Baldini, VGB Powertech 94 (3) (2014) 64–68.

[37] VDI Norm 2462 Bl. 2: Messen gasförmiger Emissionen, Bestimmung von Schwefeltrioxid in wasserdapfhaltigen Abgassen-Kondensationverfahren (Measurement of Gaseous Emissions. Determination of Sulphur Trioxide in Water Vapour containing Exhaust Gas. Condensation Method), VDI/DIN-Handbuch Reinhaltung der Luft, Band 5, Beuth Verlag, Berlin, 2011.

[38] VDI Norm 2462 Bl. 8: Messen gasförmiger Emissionen. Messen der Schwefeldioxid-Konzentration. H2O2–Thorin-Methode (Measurement of Gaseous Emissions. Measurement of the Sulfur-dioxide Concentration. $H_2O_2$–Thorin-Method)), VDI/DIN-Handbuch Reinhaltung der Luft, Band 5, Beuth Verlag, Berlin, 1985.

[39] Ya.E. Yudovich, M.P. Ketris, Int. J. Coal Geol. 67 (2006) 127–144.

[40] M. Levlin, E. Ikavalko, T. Laitinen, Fresenius J. Anal. Chem. 365 (1999) 577–586.

[41] D.H. Lim, S. Aboud, J. Wilcox, Environ. Sci. Technol. 46 (13) (2012) 7260–7266.

[42] K. Madsen, D.A. Jensen, J.F. Frandsen, R.J. Thogersen, A mechanistic study on the inhibition of the DeNO$_x$ reaction on the mercury oxidation over SCR catalysts, in: Proceedings of Air Quality VIII Conference, Arlington, October, 2011.

[43] C. Senior, Oxidation of Mercury Across SCR Catalysts in Coal-Fired Power Plants Burning Low Rank Fuels. Final Report to U.S. DOE/NETL, U. S. Department of Energy Agreement No. DE-FC26-03NT41728, Reaction Engineering International, Salt Lake City, UT, USA, 2004.

[44] H. Li, C.Y. Wu, Y. Li, J. Zhang, Environ. Sci. Technol. 45 (17) (2011) 7394–7400.

[45] D.H. Lim, J. Wilcox, Environ. Sci. Technol. 47 (2013) 8515–8522.

[46] J. Svachula, L.J. Alemany, N. Ferlazzo, P. Forzatti, E. Tronconi, F. Bregani, Ind. Eng. Chem. Res. 32 (1993) 826–834.

[47] T. Schwaemmle, B. Heidel, K. Brechtel, G. Scheffknecht, Fuel 101 (2012) 179–186.

[48] J. Dunn, H.G. Stenger Jr., I.E. Wachs, Catal. Today 51 (1999) 301–318.

[49] J. Brandenstein, H.J. Dieckmann, H. Gutberlet, VGB Powertech 88 (4) (2008) 85.